News from the CTEQ-TEA group

Pavel Nadolsky (Southern Methodist University and Michigan State University)

With the CTEQ-TEA (Tung Et. Al.) working group

China: A. Ablat, S. Dulat, Y. Fu, T.-J. Hou, I. Sitiwaldi

Mexico: A. Courtoy

USA: M. Guzzi., P. N., T.J. Hobbs, J. Huston, H.-W. Lin, D. Stump, K. Xie, C.-P. Yuan

and collaborators

Reviews of recent results in 2408.04020 (accepted by EPJP) and 2408.11131

• RESEARCH PROJECTS AND RESULTS •

https://cteq-tea.gitlab.io/

- CTEQ-TEA publications from INSPIRE
- LHAPDF grids for parton distributions
  - CT18 (N)NLO, CT18 QED, CT18 FC, …
  - Subtracted heavy-quark PDFs in the S-ACOT-MPS scheme
- Public codes
  - ePump (Hessian updating for PDFs with tolerance > 1)
  - LHAexplorer (fast surveys of data using L2 sensitivities)
  - Fantômas (Bezier parametrizations)
  - mp4lhc/mcgen (MC PDFs, combination of PDFs)
  - …

CT18up enhanced precision LHAPDF grids (2023)

On https://cteq-tea.gitlab.io/project/00pdfs/

- CT18, A, X, Z NNLO PDFs (2019 edition) presented as LHAPDF grids with a 1.9x higher number of x and Q nodes; recommended for high-mass, precision calculations, estimates of the interpolation error
- Same PDFs as in the LHAPDF library, with even more precise interpolation at $10^{-4} \leq x \leq 1$
- 2019 grids ok in other cases

Numbers of x, Q nodes in LHAPDF grids

intervals in Q	CT18	CT18up
$[Q_0, \quad m_c]$	2	4
$[m_c, \quad m_b]$	8	11
$[m_b, \quad m_t]$	14	18
$[m_t, \quad Q_{\max}]$	13	16
Total	37	49

intervals in x	CT18	CT18up	intervals in x	CT18	CT18up
$[10^{-10}, 10^{-9}]$	1	1	$[0.1, 0.2]$	7	18
$[10^{-9}, 10^{-8}]$	11	11	$[0.2, 0.3]$	6	16
$[10^{-8}, 10^{-7}]$	12	12	$[0.3, 0.4]$	5	12
$[10^{-7}, 10^{-6}]$	11	11	$[0.4, 0.5]$	3	13
$[10^{-6}, 10^{-5}]$	12	12	$[0.5, 0.6]$	6	15
$[10^{-5}, 10^{-4}]$	11	15	$[0.6, 0.7]$	6	12
$[10^{-4}, 10^{-3}]$	12	23	$[0.7, 0.8]$	8	11
$[10^{-3}, 10^{-2}]$	11	23	$[0.8, 0.9]$	14	17
$[10^{-2}, 0.1]$	12	40	$[0.9, 1]$	15	38
			Total	161	300

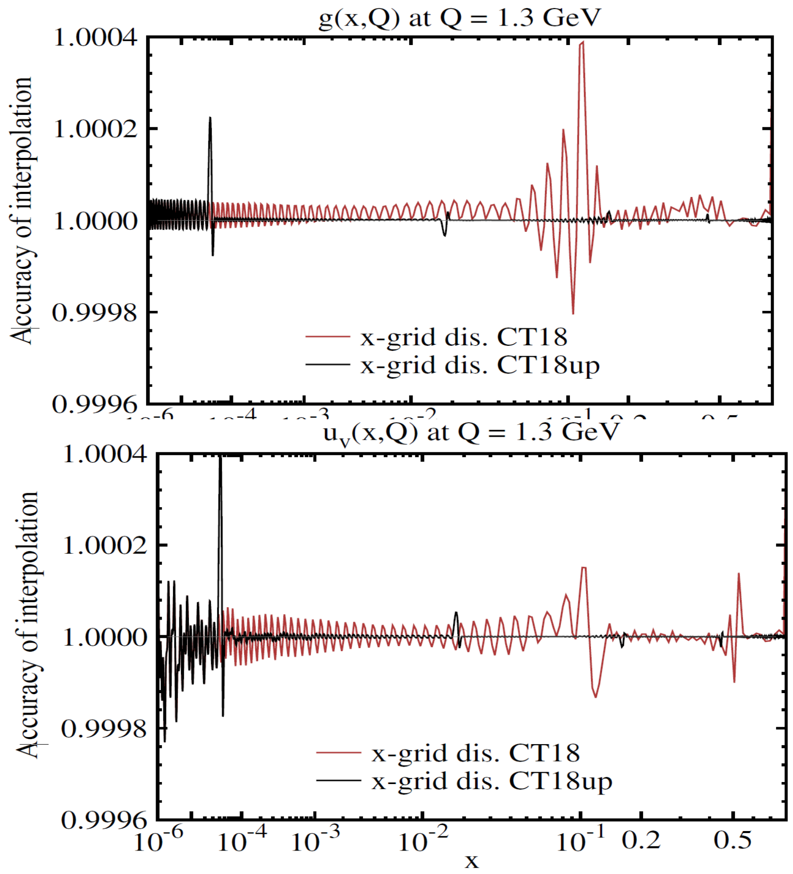

Toward a new generation of CT202X PDFs

1. Multiple preliminary NNLO fits with LHC Run-2 (di)jet, vector boson, $t\bar{t}$ data
   - based on the selections of experiments recommended in 2305.10733, 2307.11153, 2412.xxxxx
2. Next-generation PDF uncertainty quantification: Bézier curves, META combination, ML stress-testing, multi-Gaussian approaches (Mohan), …
3. Physics applications
   a. QCD+QED PDFs for a neutron (K. Xie et al., 2305.10497, talk by Hobbs)
   b. PDF dependence of forward-backward asymmetry (Y. Fu et al., 2307.07839)
   c. An L2 sensitivity study using xFitter (L. Kotz, 2401.11350)
   d. Fantômas Pion PDFs (L. Kotz et al., 2311.08447; talk by Courtoy)
   e. AI/ML models for PDF generation (Kriesten and Hobbs, 2312.02278, 2407.03411, talk by Hobbs)
   f. Residual heavy-quark PDFs for SACOT-MPS flavor at (N)NLO (2410.03876, talk by Guzzi)
4. Work on implementation of N3LO contributions

NNLO fits with new data at 8 and 13 TeV

Example

χ^2/N_{pt} for CT18+new data (CT18 in parentheses) NNLO fits; 68% CL

ID	Exp	N_{pt}	χ^2/N_{pt}
	Drell-Yan		
215	ATLAS 5.02 TeV W,Z	27	$0.82^{+0.55}_{-0.16}$ ($1.15^{+1.22}_{-0.43}$)
211	ATLAS 8 TeV W	22	$2.42^{+2.49}_{-1.51}$ ($4.25^{+6.39}_{-3.34}$)
214	ATLAS 8 TeV Z3D	188	$1.12^{+0.46}_{-0.02}$ ($1.99^{+5.10}_{-1.85}$)
212	CMS 13 TeV Z	12	$2.48^{+4.76}_{-0.88}$ ($12.03^{+38.04}_{-21.84}$)
217	LHCb 8 TeV W	14	$1.35^{+0.59}_{-0.61}$ ($1.35^{+0.72}_{-0.64}$)
218	LHCb 13 TeV Z	16	$1.18^{+1.42}_{-0.60}$ ($1.49^{+1.74}_{-0.89}$)
	13 TeV $t\bar{t}$		
521	ATLAS all-hadronic $y_{t\bar{t}}$	12	$1.06^{+0.14}_{-0.09}$ ($1.05^{+0.21}_{-0.10}$)
528	CMS dilep $y_{t\bar{t}}$	10	$1.10^{+1.08}_{-0.68}$ ($1.03^{+1.60}_{-0.74}$)
587	ATLAS lep+Jet $m_{t\bar{t}} + y_{t\bar{t}} + y^B_{t\bar{t}} + H^{t\bar{t}}_T$	34	$0.92^{+0.32}_{-0.14}$ ($0.94^{+0.59}_{-0.16}$)
581	CMS lep+jet $m_{t\bar{t}}$	15	$1.44^{+1.18}_{-0.73}$ ($1.37^{+1.86}_{-0.82}$)
	Inclusive Jet		
553	ATLAS 8 IncJet	171	$1.76^{+0.20}_{-0.12}$ ($1.80^{+0.33}_{-0.16}$)
554	ATLAS 13 IncJet	177	$1.38^{+0.13}_{-0.10}$ ($1.39^{+0.20}_{-0.11}$)
555	CMS 13 IncJet	78	$1.10^{+0.24}_{-0.17}$ ($1.11^{+0.30}_{-0.16}$)

nDY

nTT

nIncJet

nDYTTIncJet

Fits with 1 type of new data

A fit with all 3 types

PRELIMINARY

A 3-data-type fit (CT18+nDYTTIncJet)

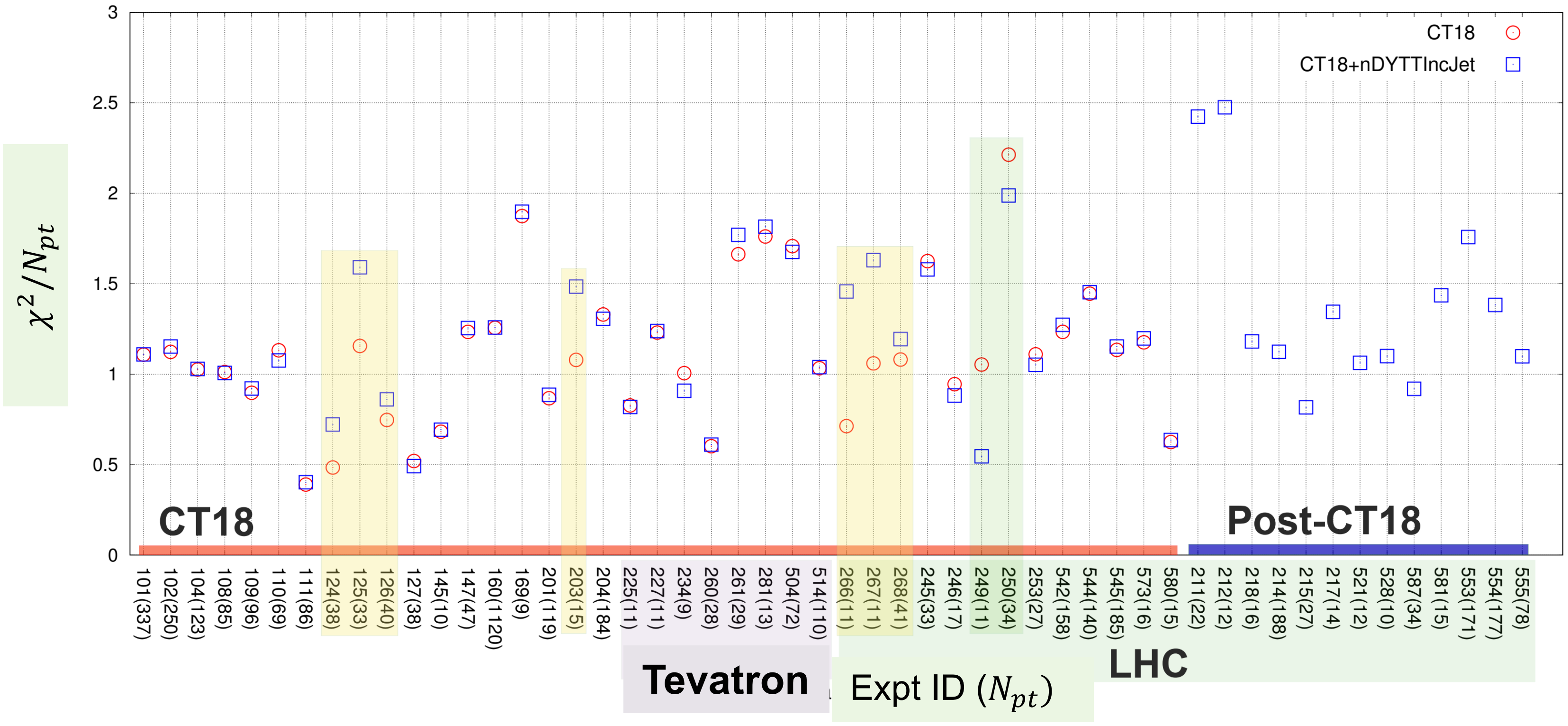

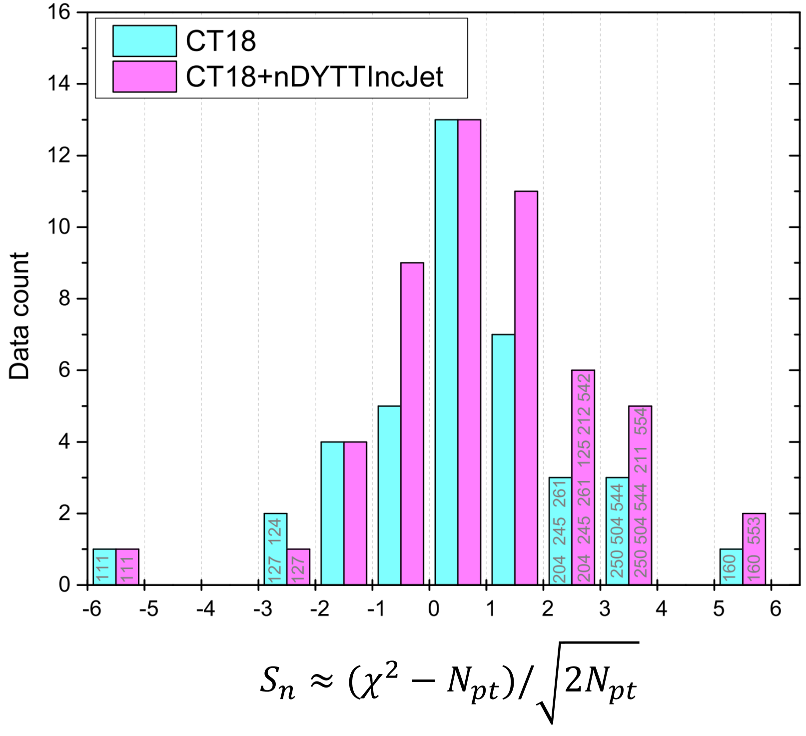

The most precise new experiments tend to have an elevated χ^2/N_{pt}, in the same pattern as observed for CT18

χ^2/N_{pt} increases for experiments 124 and 125 (NuTeV), 126 and 127 (CCFR) and 203 (E866 DY), 266 and 267 (CMS 7TeV Ach), 268 (ATLAS 7TeV W, Ach).

χ^2/N_{pt} decreases for experiments 249 (CMS 8 TeV A_{charge}), 250 (LHCb 8 TeV W/Z)

Pulls on the gluon PDF by the new data type

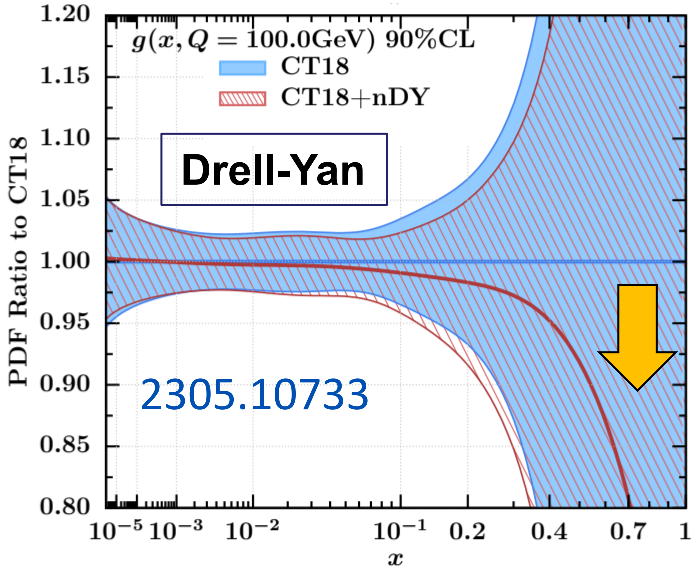

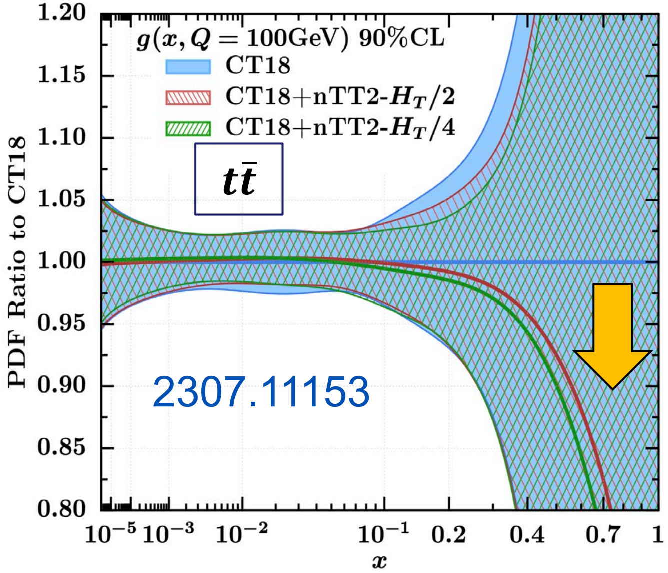

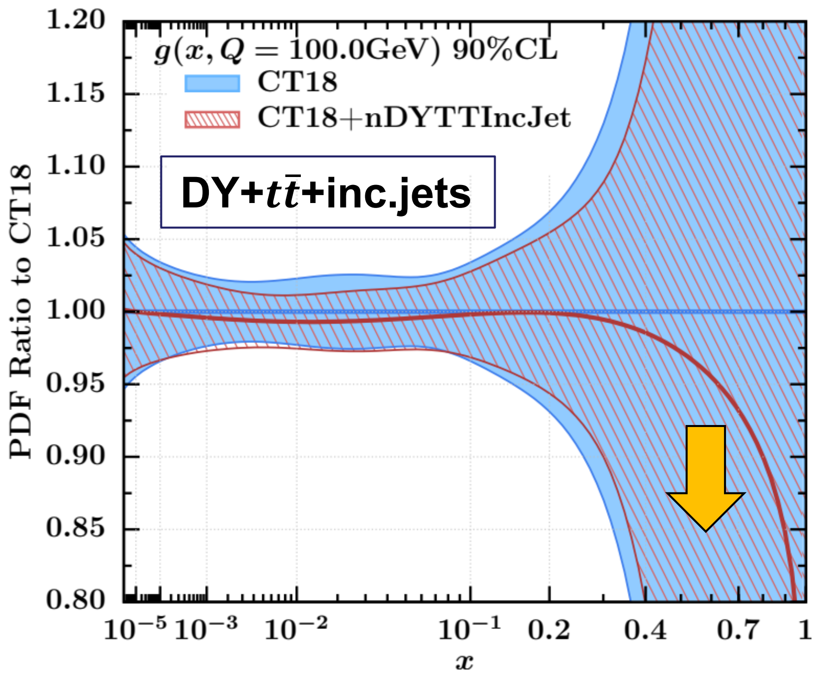

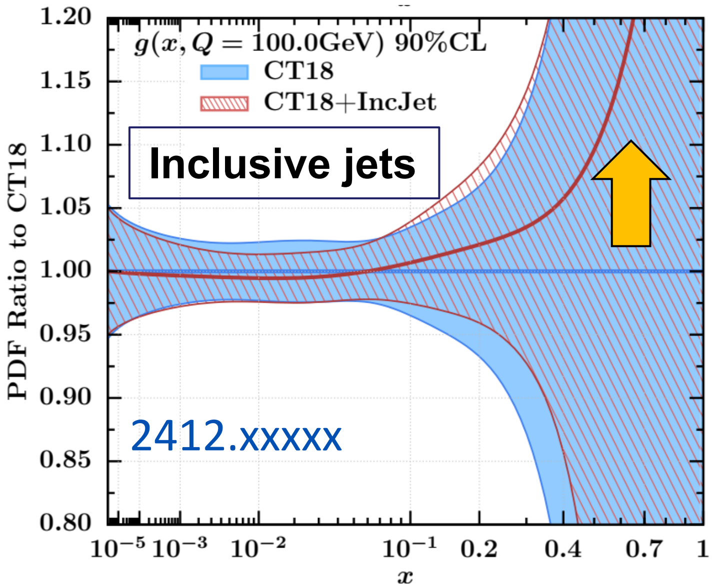

After including DY, $t\bar{t}$, and inc. jet data simultaneously, we get a softer gluon. Note that new DY and $t\bar{t}$ data favor a softer gluon, new inc. jet data prefer a harder gluon.

Mild changes in the gluon uncertainty

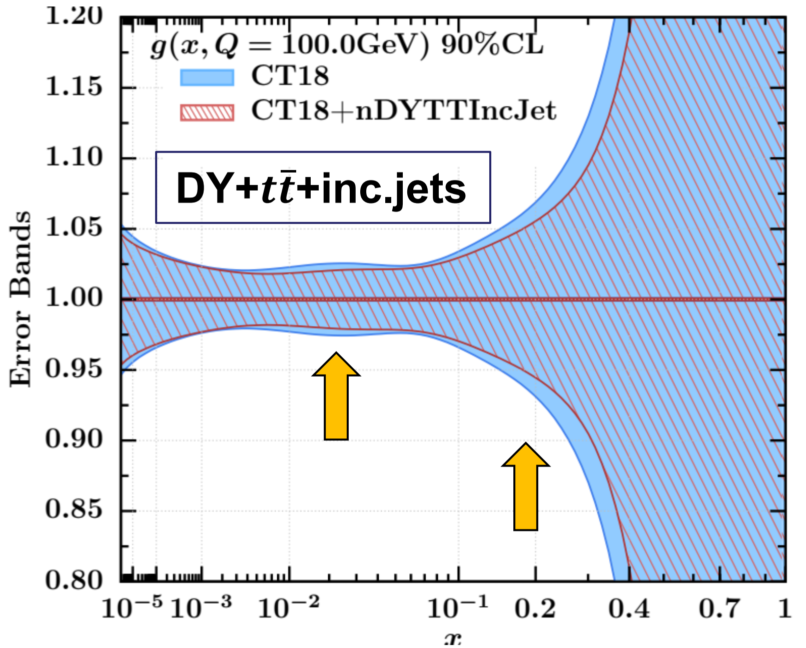

Inclusive jet vs. dijet data sets: impact on the gluon for various QCD scales

+ inclusive jets: small scale dependence, a harder $g(x, Q)$

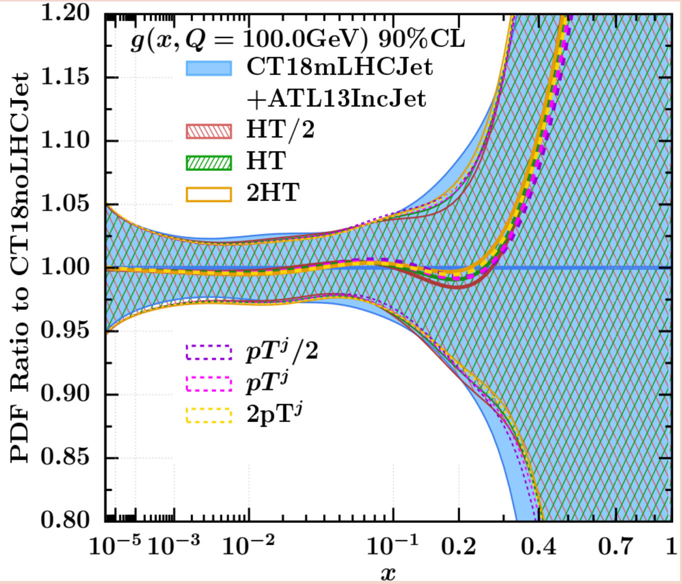

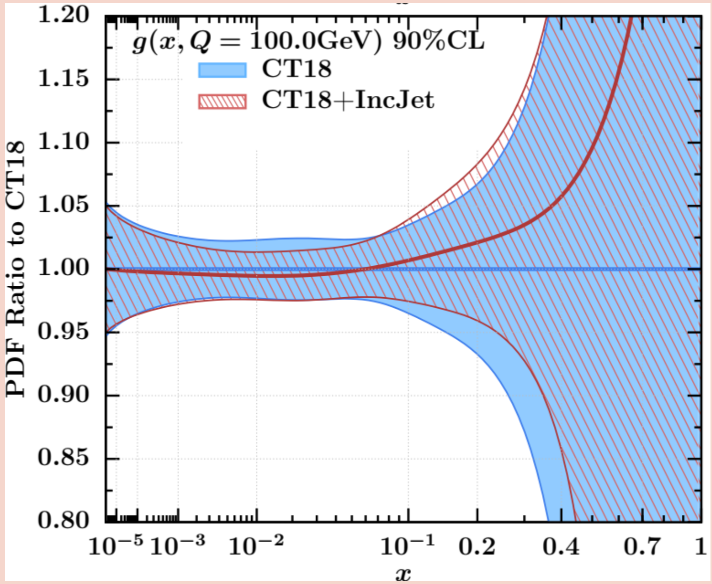

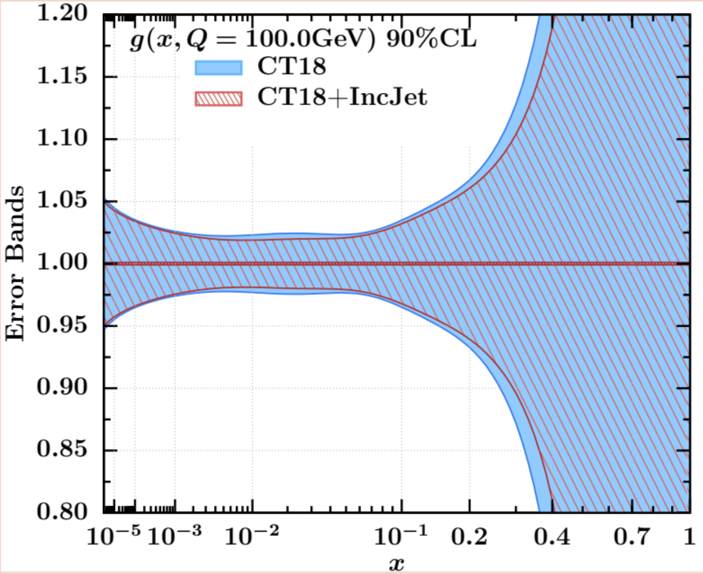

+ dijets: significant scale, dependence, varied pulls on $g(x, Q)$

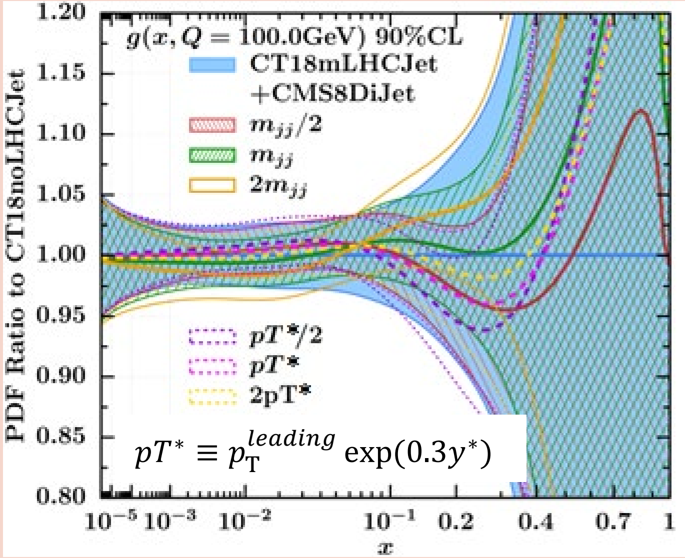

The impact of the Inc. jet data on $g(x, Q)$ is relatively independent of the scale choice. The final fit uses $\mu_{R,F} = p_T^j$, giving better χ^2.

The impact of dijet data substantially depends on scale choices, especially in the case of CMS8 TeV dijet.

Ablat et al.,2412.xxxxx (submitted)

PDFs from fits with inclusive jet and dijet data

Ablat et al.,2412.xxxxx (submitted)

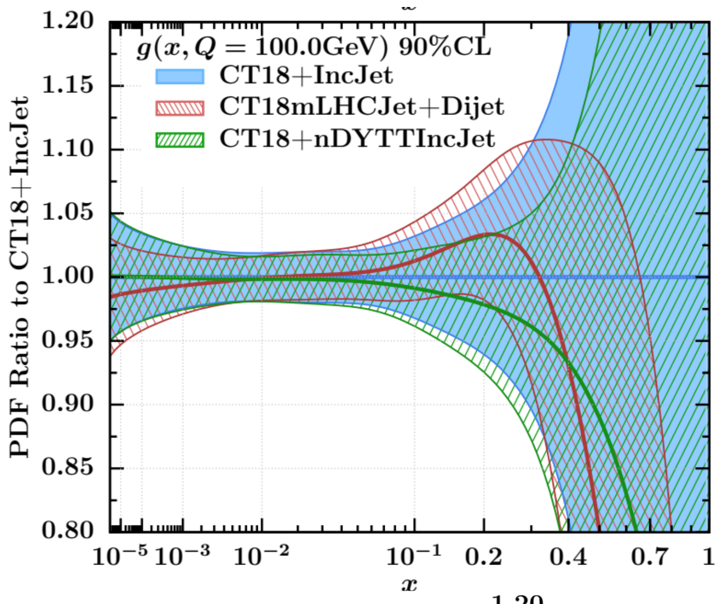

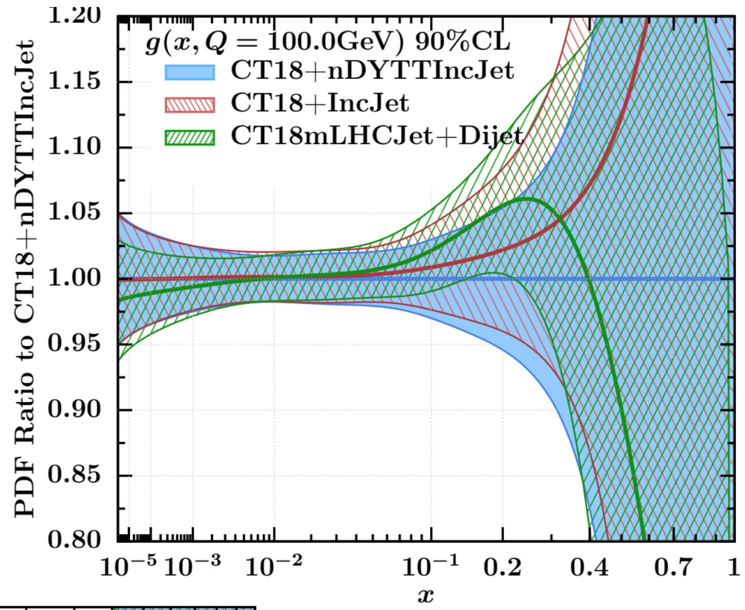

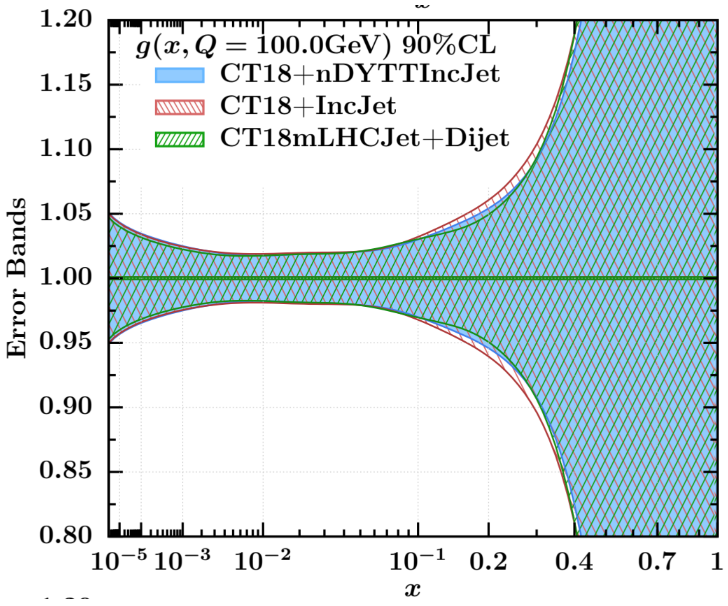

Dijet data sets tend to have larger uncertainties than inc. jets, facilitating better χ^2 for similar constraints on PDFs

χ^2/N_{pt} for fits that add one inclusive jet or dijet data set to the CT18 (without LHC jets) baseline at a time

Inclusive jets		χ^2/N_{pt} using $\mu_{R,F} \propto HT$ or p_T^j					
Experiment	N_{pt}	$HT/2$	HT	$2HT$	$p_T^j/2$	p_T^j	$2p_T^j$
ATL8IncJet	171	1.7	1.74	1.87	1.75	1.66	1.7
ATL13IncJet	177	1.42	1.36	1.4	1.52	1.31	1.28
CMS13IncJet	78	1.2	1.16	1.2	1.08	1.09	1.1
Dijets		χ^2/N_{pt} using $\mu_{R,F} \propto HT$ or $p_T^* = p_T^j \exp(0.3y^*)$					
Experiment	N_{pt}	$M_{jj}/2$	M_{jj}	$2M_{jj}$	$p_T^*/2$	p_T^*	$2p_T^*$
ATL7DiJet	90	0.81	0.79	0.87			
CMS7DiJet	54	1.55	1.55	1.63			
CMS8DiJet	122	0.95	1.2	1.9	1.25	1	1.01
ATL13DiJet	136	0.9	0.87	0.93			

Dijet data are dominated by the CMS 8 TeV dataset

Dijet data sets tend to have larger uncertainties than inc. jets, facilitating better χ^2 for similar constraints on PDFs

χ^2/N_{pt} for various treatments of NNLO/NLO K factors

TABLE III. The quality-of-fit in terms of $\chi^2/N_{\rm pt}$. Comparison of the $\chi^2/N_{\rm pt}$ values from ePump is presented, incorporating the inclusive jet datasets (ATL8IncJet, ATL13IncJet, and CMS13IncJet) sequentially on top of the CT18mLHCJet baseline. The comparison uses different theoretical treatments (NNLO, NNLOMC, SKF, SKFMC, SKFP0.5%MC) and considers scale choices such as $\hat{H}_T$ and $p_T^{\rm jet}$, along with factor-of-two variations.

Central scale	$\hat{H}_T$			$p_T^{\rm jet}$		
Variation	1/2	1	2	1/2	1	2
ATLAS 8 TeV IncJet, $N_{\rm pt} = 171$						
NNLO	3.59	2.75	2.50	6.03	3.47	2.67
NNLOMC	2.45	1.99	1.89	3.84	2.34	1.91
SKF	1.96	2.01	2.13	2.00	1.95	2.01
SKF0.5%MC	1.49	1.54	1.67	1.56	1.46	1.51
SKFMC	1.48	1.53	1.66	1.52	1.46	1.51
ATLAS 13 TeV IncJet, $N_{\rm pt} = 177$						
NNLO	3.97	2.76	2.30	7.59	3.98	2.72
NNLOMC	2.14	1.62	1.45	3.58	2.03	1.52
SKF	1.96	1.87	1.88	2.03	1.81	1.77
SKF0.5%MC	1.45	1.40	1.44	1.54	1.35	1.32
SKFMC	1.34	1.27	1.29	1.38	1.21	1.18
CMS 13 TeV IncJet, $N_{\rm pt} = 78$						
NNLO	2.57	2.04	1.87	3.92	2.47	1.98
NNLOMC	1.71	1.43	1.37	2.48	1.64	1.37
SKF	1.71	1.63	1.64	1.55	1.58	1.57
SKF0.5%MC	1.13	1.09	1.14	1.01	1.02	1.02
SKFMC	1.20	1.16	1.20	1.08	1.09	1.10

Method 1 – NNLO: Using the original NNLO theory prediction [41] alone.

Method 2 – NNLOMC: Using the NNLO theory prediction along with the MC error, and treating the latter as an uncorrelated systematic uncertainty, is an approach adopted by NNPDF [69, 70].

Method 3 – SKF: Using the smooth NNLO K-factor. This method was adopted by MSHT [54] group.

Method 4 – SKF0.5%MC: Using the smooth NNLO K-factor, we include an additional 0.5% MC error in the theory prediction, treating it as an uncorrelated systematic uncertainty. This approach was adopted in the CT18 analysis [1].

Method 5 – SKFMC: In addition to using the smooth NNLO K-factor, we incorporate the MC uncertainty extracted from the grid [41], treating it as an uncorrelated systematic error. This approach forms the basis of our final results.

More than one plausible treatment of theo. and expt. syst. errors (decorrelations, K-fac smoothing, …) sizeably changes χ^2/N_{pt}, with less effect on the resulting PDFs

An ATLAS, CTEQ-TEA, and MSHT comparative study of NNLO and aN3LO PDF sensitivities

X.Jing et al.,arXiv:2306.03918

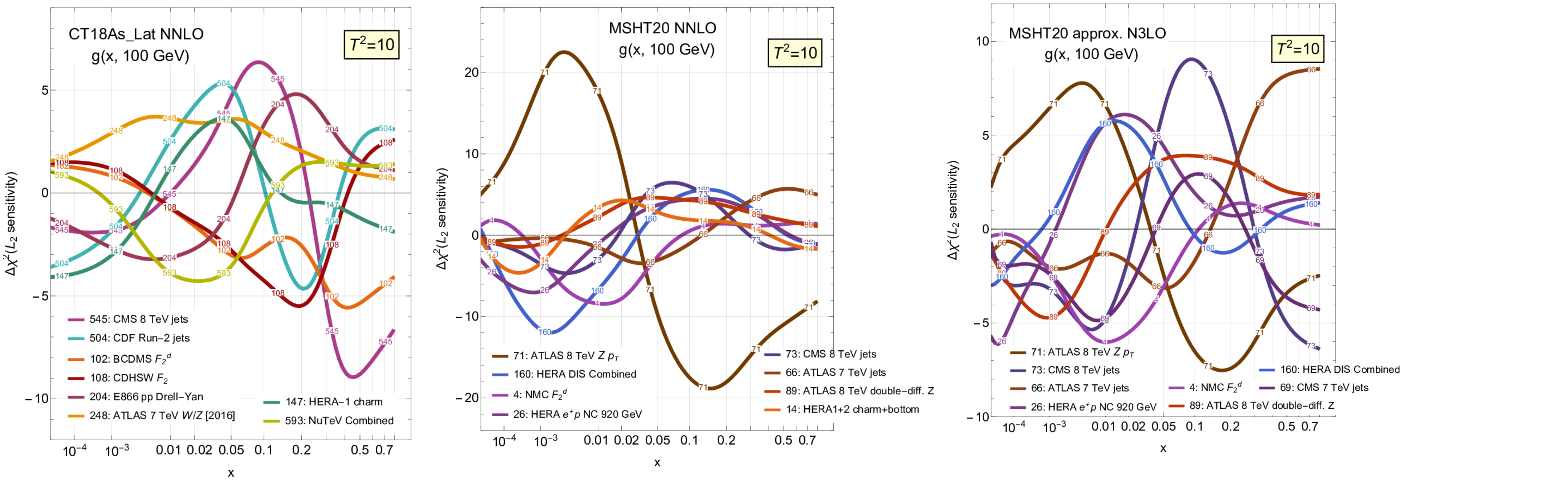

- Comparisons of constraints from individual data sets using the common L_2 sensitivity metric. [Here, pulls on the gluon in NNLO and aN3LO analyses.]
- An interactive website (https://metapdf.hepforge.org/L2/) to plot such comparisons

[2070 figures in total; a code L2LHAexplorer to plot L2 sensitivities for LHAPDF grids]

L. Kotz, 2401.11350

xFitter+L2LHAexplorer

L2 sensitivities were computed using xFitter

- PDF sets (NNLO, $\alpha_s(M_Z) = 0.118$, $Q = 2\ \mathrm{GeV}$, $T^2 = 10$):
  - CT18
  - CT18As
  - MSHT20
- Data sets (included in xFitter):
  - ATLAS Drell-Yan ($\sqrt{s} = 7\ \mathrm{TeV}$)
  - ATLAS jet production ($\sqrt{s} = 2.76\ \mathrm{TeV}$)
  - CMS W+c production ($\sqrt{s} = 7\ \mathrm{TeV}$)
  - H1+ZEUS combined *c* and *b* production
  - H1 jet production
  - HERA I+II DIS
  - LHCb *c* and *b* production ($\sqrt{s} = 7\ \mathrm{TeV}$)
  - ZEUS jet production

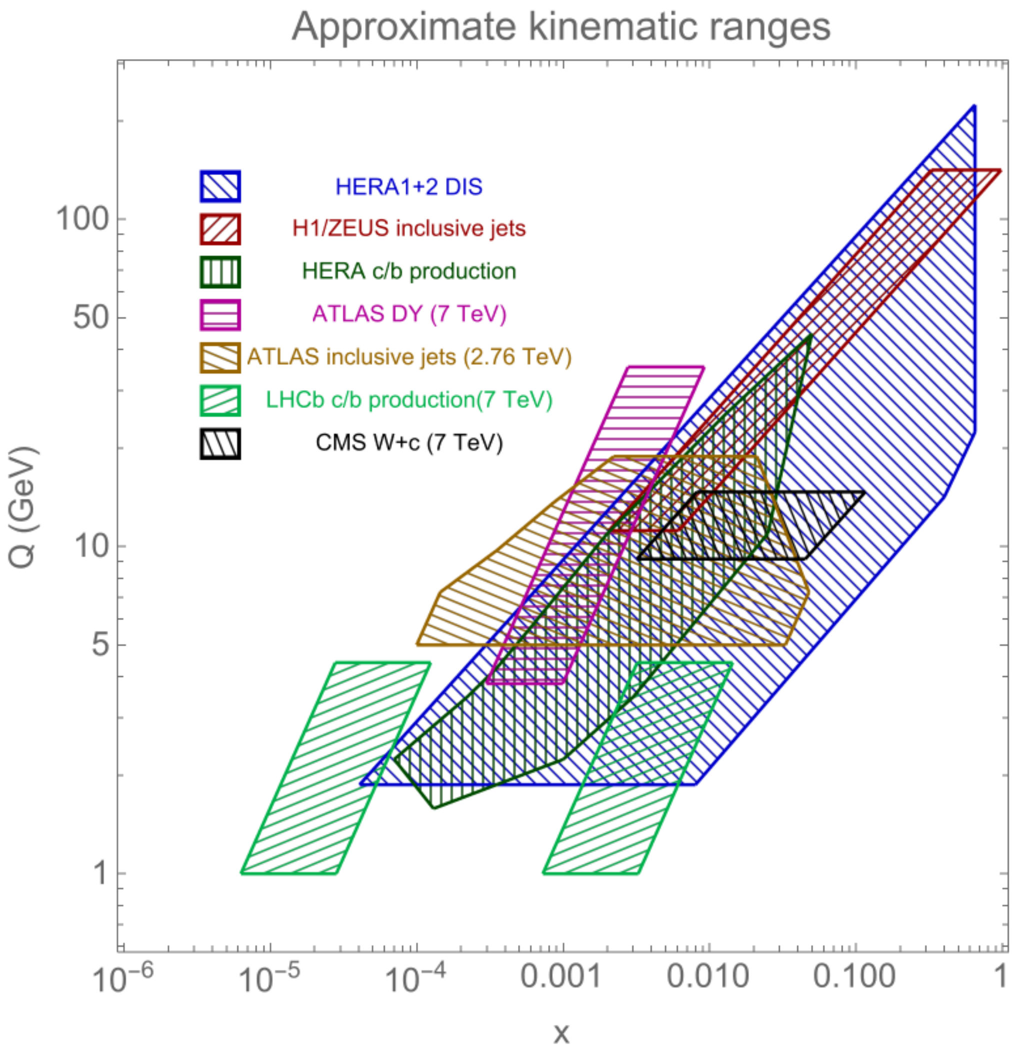

HERA I+II combined inclusive DIS [in CT18 and MSHT20]

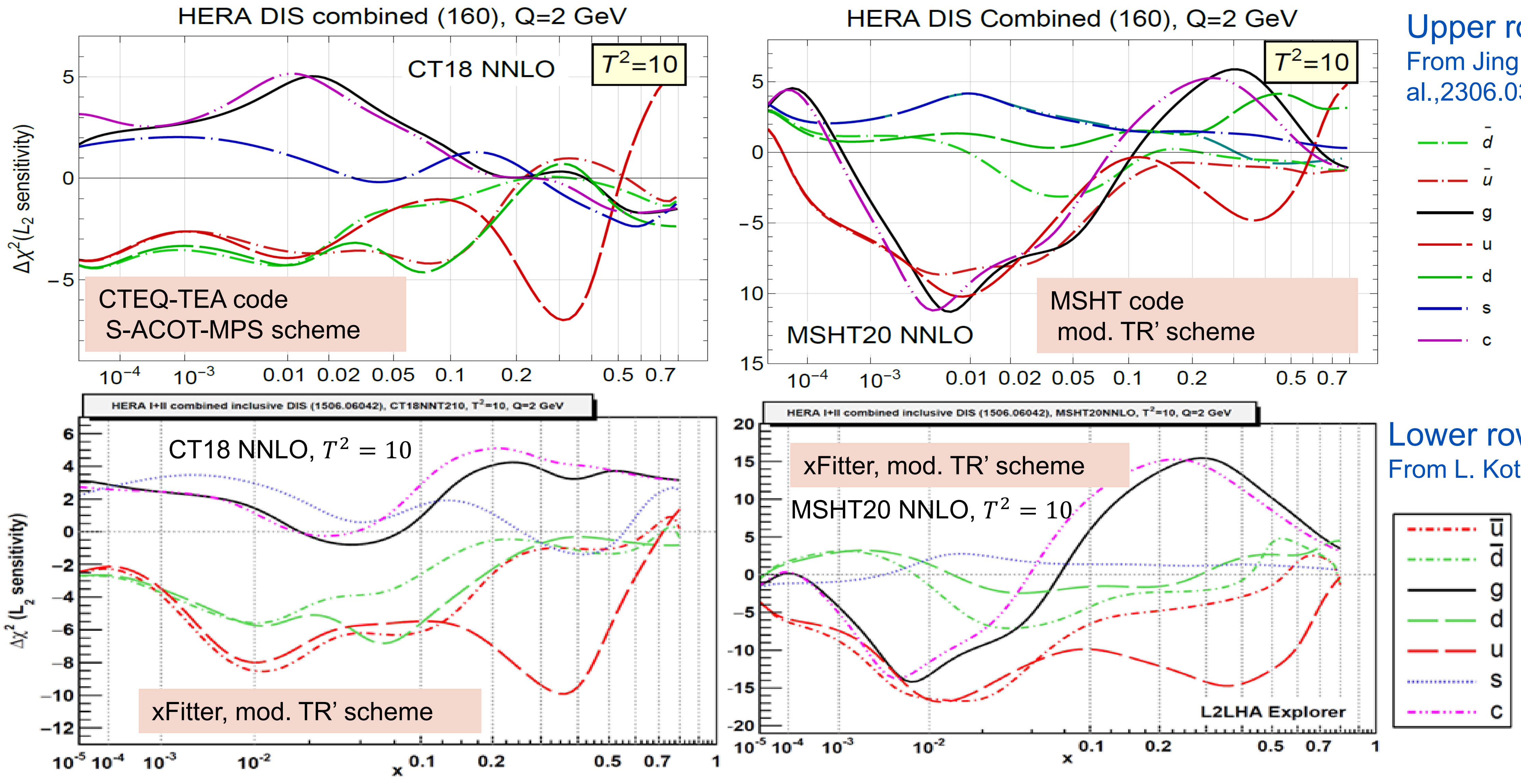

Upper row:
From Jing et al.,2306.03918

Lower row:
From L. Kotz, 2401.11350

Left column: differences in χ^2 definition and heavy-quark scheme. Same PDFs and m_Q.

Right column: differences in χ^2 definition only. Same PDFs and m_Q.

Correlations with PDFs in PVDIS at JLab 22 GeV

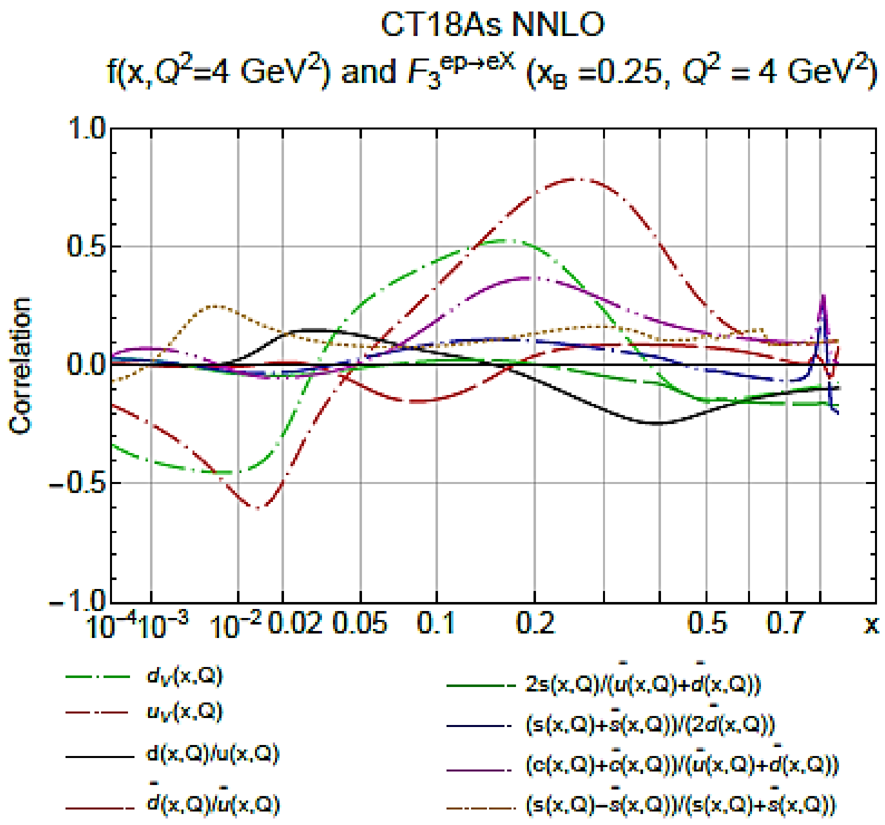

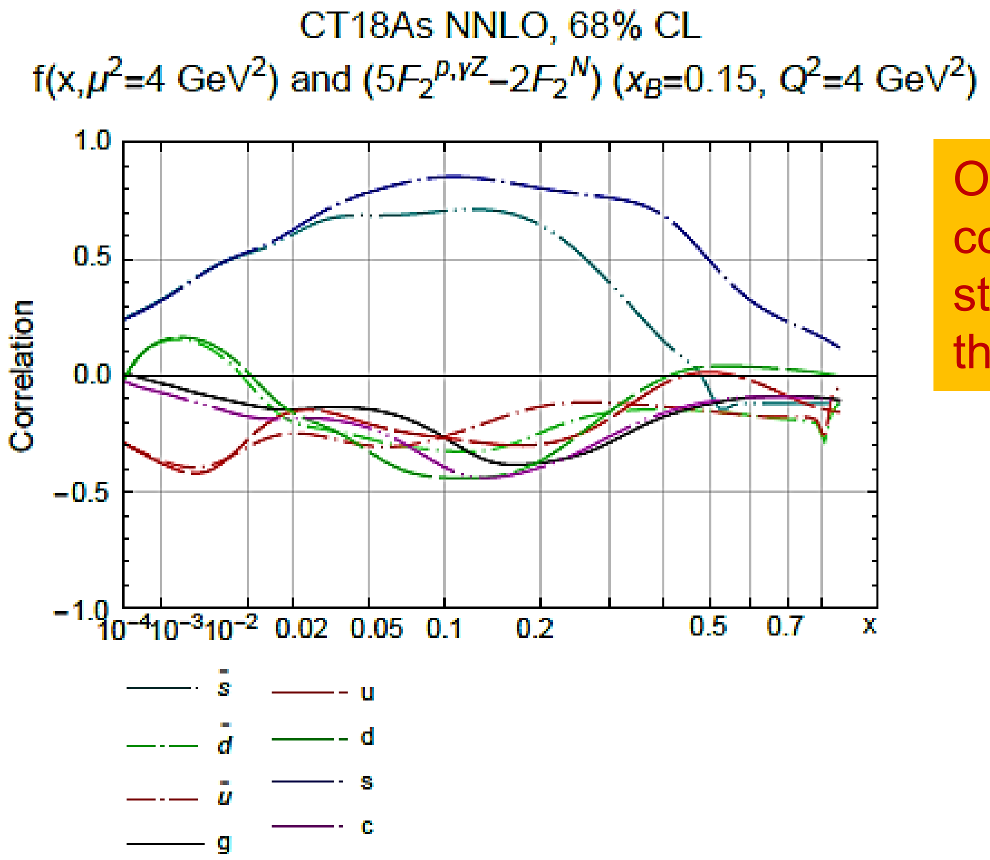

arXiv:2306.09360
arXiv:2408.04020

Observe a large correlation of PVDIS with strangeness; how large is the actual data sensitivity?

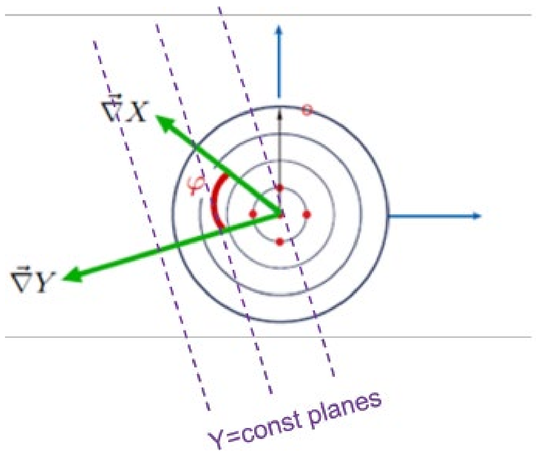

Figure 16: When combined with other high-energy observables in a QCD global fit, parity-violating lepton scattering may access unique quark charge-flavor currents to help disentangle the flavor dependence of the nuclear sea at high x. In the upper row, we plot the Hessian correlations of (a) several PDF flavor combinations with the parity-violating structure function $F_3(x_B, Q)$ and (b) the individual PDF flavors and a combination $5F_2^{\gamma Z,p}(x_B, Q) - 2F_2^N(x_B, Q)$ with a potential sensitivity to strangeness. (c) We illustrate

Sensitivities to PDFs in PVDIS at JLab 22 GeV

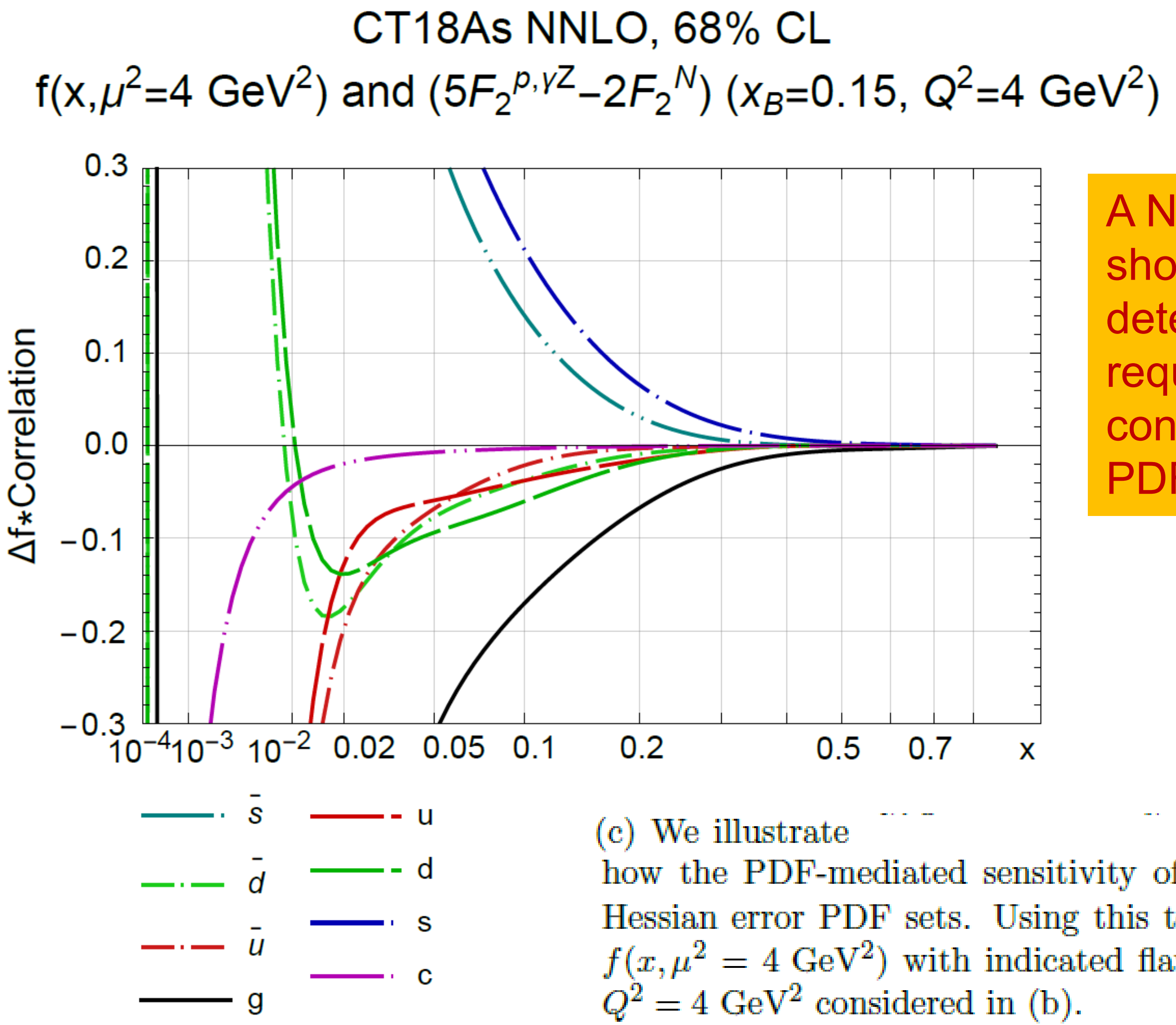

arXiv:2408.04020

A NEW TECHNIQUE; shows that PVDIS determination of strangeness requires tight external constraints on gluon and dbar PDFs

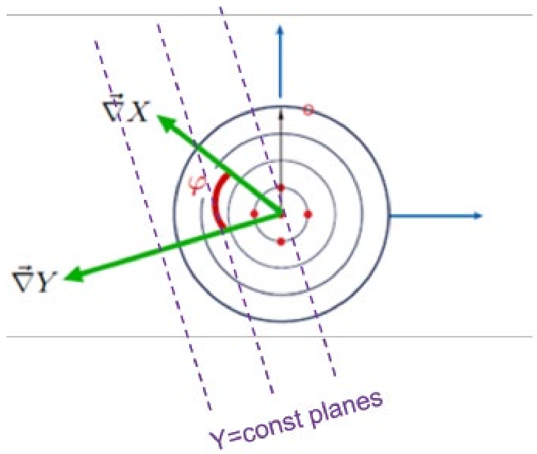

(c) We illustrate ... how the PDF-mediated sensitivity of Y to X can be estimated using the gradients computed with the Hessian error PDF sets. Using this technique, panel (d) estimates the sensitivity of constraints on PDFs $f(x, \mu^2 = 4\ \mathrm{GeV}^2)$ with indicated flavors to the combination $5F_2^{\gamma Z,p}(x_B, Q) - 2F_2^N(x_B, Q)$ at $x_B = 0.15$, $Q^2 = 4\ \mathrm{GeV}^2$ considered in (b).

Second-order corrections to the Hessian formalism

W. Zhan et al., arXiv: 2411.11645; T-J. Hou et al., arXiv:1607.06066

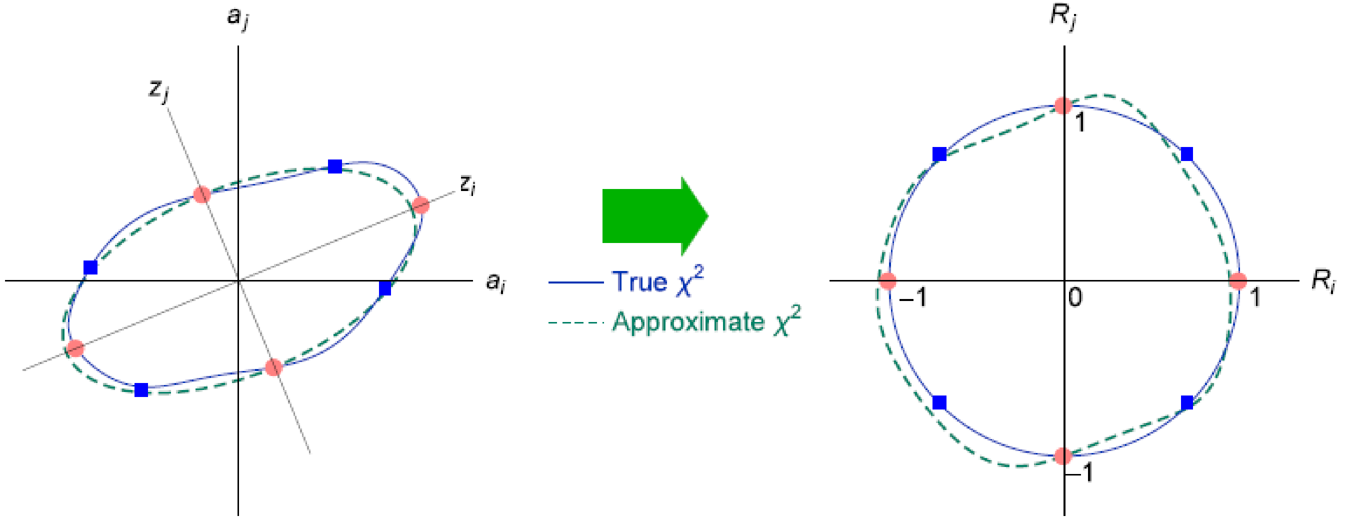

FIG. 1: Contours of constant χ^2 under the scaling transformation of PDF parameters.

The second-order correction requires $\frac{N_{par}(N_{par}-1)}{2}$ Hessian PDFs evaluated at off-diagonal points (blue squares)

$$X_{\pm i,\pm j} \equiv X\left(0, ..., R_i = \pm\frac{1}{\sqrt{2}}, ..., R_j = \pm\frac{1}{\sqrt{2}}, ..., 0\right)$$

The new study investigates such corrections with pseudodata. The 2nd order correction can be sizeable with moderately precise data.

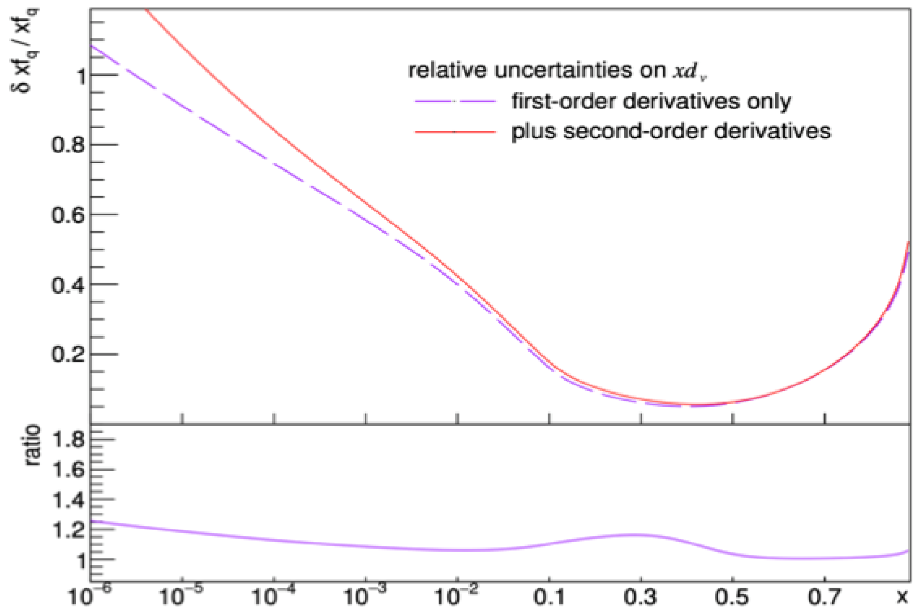

For an observable X, use the Taylor series to estimate non-linear corrections to the Hessian PDF uncertainty:

$$X(\vec{R}) = X_0 + \sum_{i=1}^{D}\frac{\partial X}{\partial R_i}R_i + \frac{1}{2}\sum_{i,j=1}^{D}\frac{\partial^2 X}{\partial R_i \partial R_j}R_i R_j + \ldots .$$

The derivatives can be estimated by finite differences,

$$\frac{\partial X}{\partial R_i} \approx \frac{X_{+i} - X_{-i}}{2},$$
$$\frac{\partial^2 X}{\partial R_i^2} \approx X_{+i} + X_{-i} - 2X_0,$$
$$\frac{\partial^2 X}{\partial R_i \partial R_j} \approx \frac{X_{+i,+j} + X_{-i,-j} - X_{+i,-j} - X_{-i,+j}}{2}.$$

THANK YOU FOR YOUR ATTENTION!